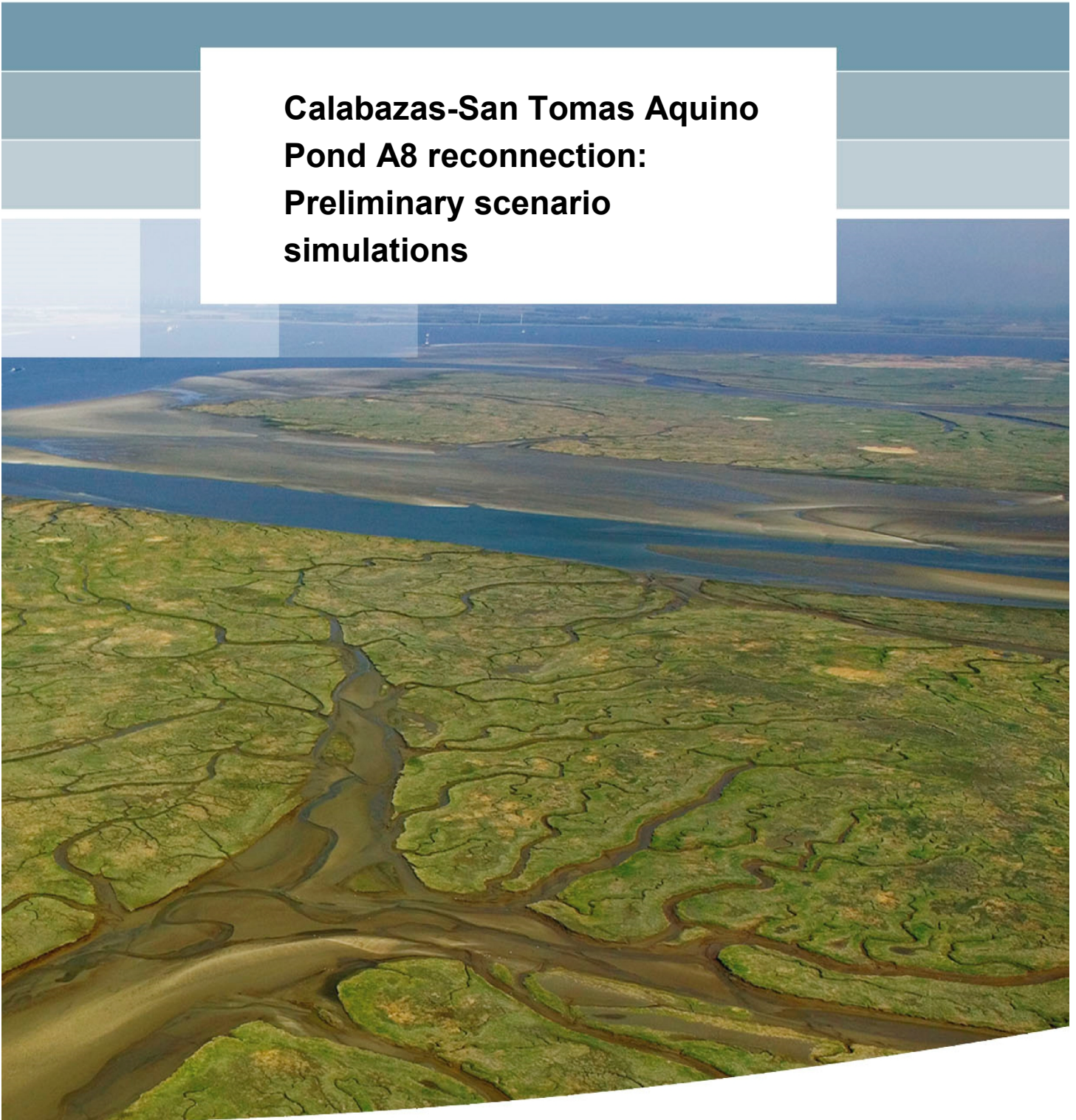


**Calabazas-San Tomas Aquino
Pond A8 reconnection:
Preliminary scenario
simulations**



**Calabazas-San Tomas Aquino Pond
A8 reconnection: Preliminary
scenario simulations**

Björn R. Röbbke
Mick van der Wegen

11200020-002

Title
 Calabazas-San Tomas Aquino Pond A8
 reconnection: Preliminary scenario simulations

Client	Project	Reference	Pages
Santa Clara Valley Water District	11200020-002	11200020-002-ZKS-0003	15

Keywords

Calabazas Creek, San Tomás Aquino Creek, Pond A8, South San Francisco Bay, Santa Clara Valley Water District, South Bay Salt Pond (SBSP) Restoration Project, creek reconnection, hydrodynamic and morphodynamic simulations, Delft3D-FM

Summary

Within the restoration of the South San Francisco Bay (western USA), the Santa Clara Valley Water District is exploring to reconnect two creeks of the Alviso Complex, i.e. the Calabazas and San Tomás Aquino Creeks, with the adjacent Pond A8. In this study, the hydro- and morphodynamic effects of two reconnection scenarios (single and double breaching) are investigated based on preliminary simulations for a time scale of 5 ½ years using a two-dimensional Delft3D Flexible Mesh model.

The simulation results demonstrate that both reconnection scenarios for Calabazas and San Tomás Aquino Creeks have a significant impact on the local hydro- and morphodynamics. In particular the downstream flow velocities during high river discharge events greatly increase once the creeks are reconnected to Pond A8. This can be especially observed in the double breaching scenario. The larger flow velocities in the reconnection scenarios are directly linked to an increase in the sediment transport capacity in both creeks, which in turn causes more erosion/less deposition indicating an increase in the sediment export (particularly in case of the double breaching). Directly to the north of the breaches, significant fan creation can be observed in the model in both scenarios.

The larger flow velocities during high discharges in Calabazas and San Tomás Aquino Creeks in the reconnection scenarios can be assumed to reduce the regional flooding risk originating from creek discharge. Furthermore, the indicated increase in sediment export by the creeks may lead to the conclusion that the breaching reduces the dredging volumes especially in the lower creeks, which are currently required to maintain the flow capacity. However, further simulations have to be performed in order to make more reliable and quantitative predictions on the hydro- and morphodynamic impact of the various reconnection scenarios and on the expected future flooding risk and required dredging volumes.

Version	Date	Authors	Initials	Review	Initials	Approval	Initials
1.2	Jan. 2018	Björn R. Röbbke Mick van der Wegen	<i>B.R.</i>	Julia Vroom	<i>JV</i>	Dirk-Jan Walstra	<i>DJW</i>

Contents

List of figures and tables	iii
1 Introduction	1
2 Study aims	3
3 Methods	5
4 Results	9
5 Discussion and conclusions	13
References	15

List of figures and tables

Figure 1.1: Satellite image of South San Francisco Bay and the Alviso Complex.

Figure 3.1: Aerial views of the study area including the computational mesh of the two-dimensional D3D FM model employed in this study.

Figure 3.2: Relation between the discharge Q_{inst} and the suspended sediment concentrations C_{sus} measured between 10/10/2011 and 10/03/2017 for Guadalupe River and Coyote Creek.

Figure 3.3: Bed elevations of Pond A8 and the downstream areas of Calabazas and San Tomás Aquino Creeks in the reference case, and reconnection Scenarios A and B.

Figure 4.1: Depth averaged flow velocities for cross section Cal simulated in the reference case, and Scenarios A and B.

Figure 4.2: Depth averaged flow velocities for cross section STA simulated in the reference case, and Scenarios A and B.

Figure 4.3: Suspended sediment transport through cross sections Cal and STA simulated for the reference case, Scenarios A and B during three high river discharge events in January 2017.

Figure 4.4: Simulated cumulative erosion and sedimentation after 5 ½ years for the reference case, and reconnection Scenarios A and B.

Figure 4.5: Differences in bed elevations after 5 ½ years between Scenario A and the reference case, and between Scenario B and the reference case.

Table 3.1: Overview of the gauge stations which were used to derive the discharge boundary conditions for various creeks in the study area.

Table 3.2: Overview of the morphodynamic simulations computed with the Delft3D Flexible Mesh model of the Alviso Complex.

1 Introduction

During the last 150 years, salt mining, urbanisation and agriculture have resulted in the loss of more than 80 % of the natural tidal wetlands in the southern San Francisco Bay (western USA; FOXGROVER et al. 2004). This loss has been particularly severe in the southern part of the bay. In 2008, the California Department of Fish and Game, the U.S. Fish and Wildlife Service and the California Coastal Conservancy launched the South Bay Salt Pond (SBSP) Restoration Project, in order to restore about 60 km² of industrial salt ponds in the southern San Francisco Bay to natural mixed wetland habitats. Additional goals of the SBSP project are to provide wildlife-oriented public access and recreation and to improve the local flood management (http://www.southbayrestoration.org/Project_Description.html).

This study focuses on the Alviso Complex, which is located in the southernmost part of the San Francisco Bay (Figure 1.1). The Alviso Complex is a mud-dominated area comprising numerous ponds and creeks that are partly connected to each other (FOXGROVER et al. 2007; FOXGROVER et al. 2014). The area is dominated by a mixed semidiurnal tide (maximum tidal range circa 3.6 m) propagating several kilometres inland at creeks and sloughs (SHELLENBARGER et al. 2015). Being characterised by a periodic discharge regime, most of the creeks



Figure 1.1: Satellite image of South San Francisco Bay and the Alviso Complex including the main creeks and the extent of Pond A8. Calabazas and San Tomás Aquino Creeks are planned to be reconnected with Pond A8 (red circles) in order to restore wetlands, reduce the local flood risk and to reduce the dredging volumes currently required to maintain the flow capacity.

fall dry during the hydrological summer (spring till autumn), while high river discharge occurs particularly during the hydrological winter (autumn till spring; SHELLNBARGER et al. 2015).

The Santa Clara Valley Water District is exploring reconnecting two creeks of the Alviso Complex, i.e. the Calabazas and San Tomás Aquino Creeks, with the adjacent Pond A8 (Figure 1.1). The reconnection is intended to (i) restore the wetlands in the Pond A8 complex, (ii) mitigate the local flood risk and (iii) reduce the hydraulic inefficiencies due to the channelisation of the creeks and by this to reduce the high dredging volumes currently required to maintain the flow capacity and to avoid flooding in the winter season.

2 Study aims

In this study, the effects of the creek reconnection on the local hydrodynamics, sediment transport and morphodynamics are investigated with preliminary numerical simulations using the Delft3D Flexible Mesh (D3D FM) suite developed by the Dutch institute Deltares. Based on a hydro- and morphodynamic two-dimensional D3D FM model of the wider study area and a time scale of about 5 ½ years, two potential reconnection scenarios are simulated and compared with the reference case (i.e. the current situation without reconnections). The study particularly focuses on the effects of the reconnection on (i) the tidal signal and flow velocities in the downstream parts of Calabazas and San Tomás Aquino Creeks, (ii) the erosion-sedimentation pattern in the creeks as well as (iii) the morphodynamics (esp. fan creation) in Pond A8. Owing to a limited sensitivity analysis, the study provides qualitative rather than quantitative insights.

3 Methods

The D3D FM model used in this study is based on the Alviso Slough D3D FM model by REY (2015), which has been calibrated and validated using water depths, flow velocities, discharges as well as suspended sediment concentrations measured in 2012. In order to simulate the reconnection scenarios, the model has been extended to include the Sunnyvale East Channel, Calabazas Creek and San Tomás Aquino Creek. The resulting model domain reaches from the southernmost San Francisco Bay in the north to Highway 101 in the south (Figure 3.1a and b). The computational mesh consists of triangular and rectangular cells with a maximum resolution of about 10 m and 4 m respectively in the area of interest (Figure 3.1c). Consequently, the cross-stream profiles of both Calabazas and San Tomás Aquino Creeks are covered by at least 5 mesh cells. The bed level of the model is derived from USGS LIDAR and USGS bathymetry survey base line data from the year 2010.

The hydrodynamic offshore boundary conditions of the model are based on water levels according to 26 tidal components. The tidal components were derived from measured water levels at Coyote Creek station in the period between 2011 and 2015 (Station ID: 9414575; <https://tidesandcurrents.noaa.gov/stationhome.html?id=9414575>). For the upstream boundaries of the creeks, discharge boundary conditions are used. These are derived from measurements taken between 10/10/2011 and 10/03/2017 at various gauge stations by the Santa Clara Valley Water District (Table 3.1).

The model considers mud only ($\varnothing < 63 \mu\text{m}$), which is the dominant grain size in the study area. The sediment transport formulations are based on VAN RIJN (1993). Both the initial sediment thickness (3 m) and the bottom roughness (Manning's $n = 0.026$) are uniform throughout the domain.

All model runs are performed in 2D mode. Based on an explicit scheme, the model uses a time-varying computational time step (between 1 s and 20 s) to achieve a Courant number of 0.7 (Deltares 2016). Bed level changes within the model domain are updated after every time step (morphodynamic simulations). Dredging of the creeks is not implemented in the model.

An important input to the D3D FM model is the sediment load at the upstream boundaries of the main creeks in the domain. While measured mud concentrations are available for Guadalupe River and Coyote Creek, no corresponding data exist for the Calabazas and San Tomás Aquino Creeks. Therefore, sediment loads for these creeks were derived from the relation between the discharge Q_{inst} and the suspended sediment concentrations C_{sus} measured between 10/10/2011 and 10/03/2017 for the nearby Guadalupe River and Coyote Creeks

Table 3.1: Overview of the gauge stations which were used to derive the discharge boundary conditions for various creeks in the study area.

Channel/Creek/River	Gauge station
Sunnyvale East Channel	Station number 74 (at Hwy 101)
Calabazas Creek	Station number 26.1 (at Wilcox School)
San Tomás Aquino Creek	Station number 28 (At Mission College Blvd.)
Guadalupe River	Station number 109 (USGS ID 11169025; at Hwy 101)
Coyote Creek	Station number 97 (USGS ID 11172175; at Hwy 237)

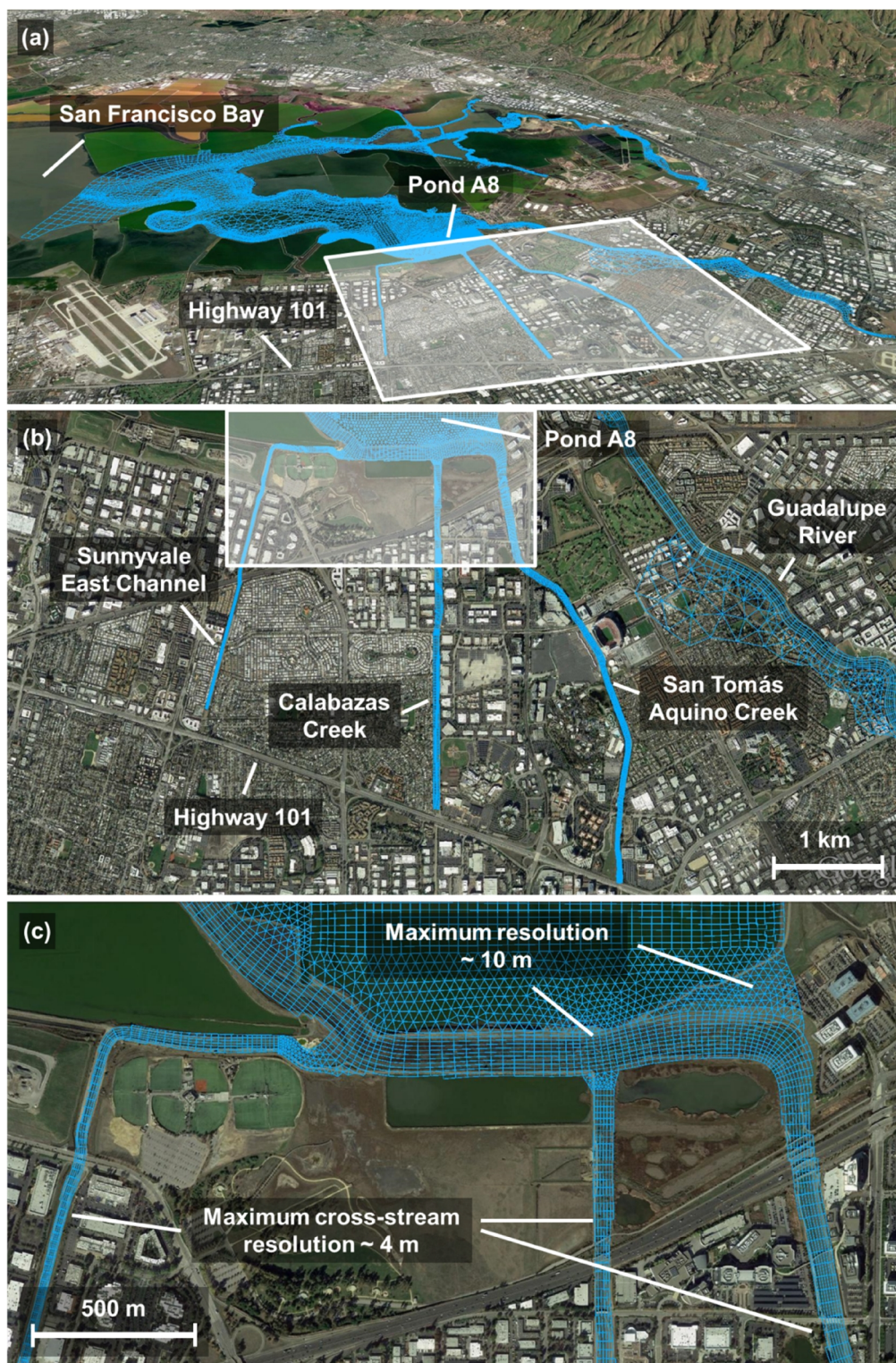


Figure 3.1: Aerial views of the study area including the computational mesh of the two-dimensional D3D FM model employed in this study. The model is used to simulate two reconnection scenarios, in which Calabazas and San Tomás Aquino Creeks are reconnected with Pond A8. The computational mesh is based on a combination of triangular and rectangular cells with a maximum resolution of about 10 m and 4 m respectively.

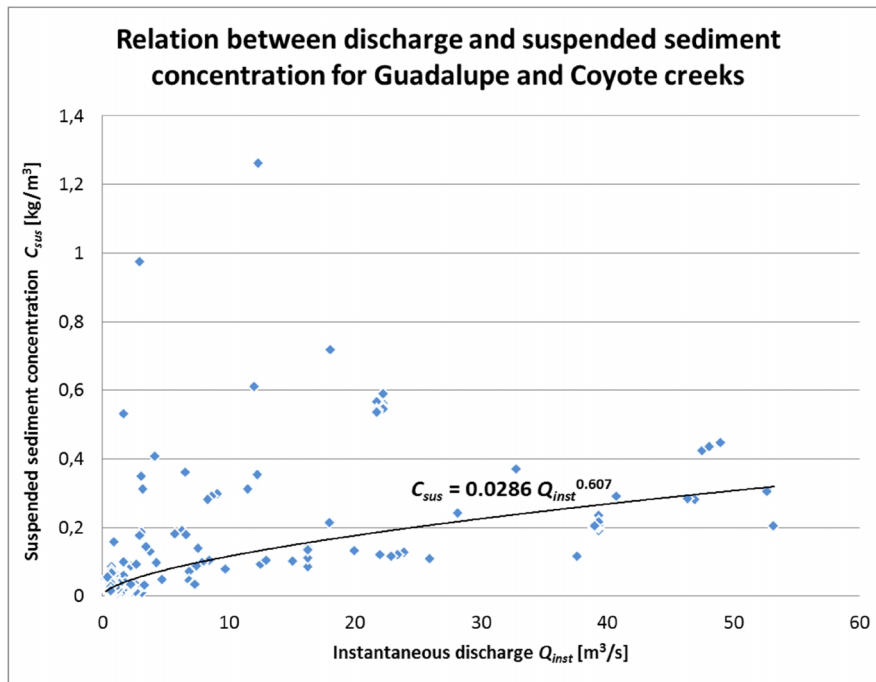


Figure 3.2: Relation between the discharge Q_{inst} and the suspended sediment concentrations C_{sus} measured between 10/10/2011 and 10/03/2017 for Guadalupe River and Coyote Creek. Based on this relation, sediment loads for the Sunnyvale East Channel and the Calabazas and San Tomás Aquino Creeks were derived.

(Figure 3.2). Based on this relation ($C_{sus} = 0.0286 Q_{inst}^{0.607}$) and the discharges measured for the two creeks, suspended sediment concentrations of between 0.2 kg/m^3 and 0.4 kg/m^3 during high river discharges were determined for Calabazas and San Tomás Aquino Creeks. These values are in the order of measured sediment loads from other creeks in the wider study area (see SHELLENBERGER et al. 2015).

In this study, the reference case (continuation of the current configuration; Figure 3.3a) as well as two potential reconnection scenarios (Figure 3.3b and c) are simulated with the D3D FM model. In reconnection Scenario A, Calabazas and San Tomás Aquino Creeks are re-connected to Pond A8 by breaching the levee directly north to the confluence of both creeks.

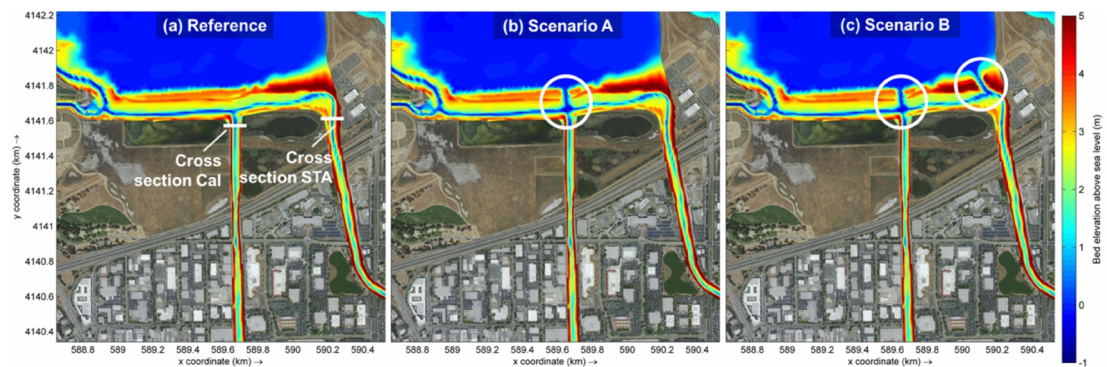


Figure 3.3: Bed elevations of Pond A8 and the downstream areas of Calabazas and San Tomás Aquino Creeks in the reference case (a) and reconnection Scenarios A (b) and B (c). The white lines in (a) mark the locations of two cross sections in the downstream parts of Calabazas and San Tomás Aquino Creeks where simulation results are presented in Chapter 4.

In reconnection Scenario B, a second levee breach is added 600 m further upstream where San Tomás Aquino Creek sharply turns. Based on these configurations and the hydrodynamic periods 10/10/2015–10/03/2017 (short-term) and 10/10/2011–10/03/2017 (longer-term), altogether six simulations have been performed with the D3D FM model (Table 3.2).

Table 3.2: Overview of the morphodynamic simulations computed with the Delft3D Flexible Mesh model of the Alviso Complex.

	Reference case	Scenario A – 1 Breach	Scenario B – 2 Breaches
short-term (1 ½ years)	Oct 2015–Mar 2017	Oct 2015–Mar 2017	Oct 2015–Mar 2017
longer-term (5 ½ years)	Oct 2012–Mar 2017	Oct 2012–Mar 2017	Oct 2012–Mar 2017

4 Results

Generally, both the short-term (1 ½ years) and the longer-term (5 ½ years) simulations show similar trends in the computed hydro- and morphodynamics. Therefore, only the results of the longer-term simulations are presented and discussed.

Both reconnection scenarios have a significant impact on the simulated hydrodynamics in the study area. This is clearly indicated by the depth averaged flow velocities simulated for the lower Calabazas and San Tomás Aquino Creeks in the reference case and the two scenarios at the cross sections illustrated in Figure 3.3. Figure 4.1a shows that the flow velocities during high discharges in Calabazas Creek increase by a factor of up to 4 in Scenario A and by a factor of maximum 4.5 in Scenario B compared to the reference case. Also the tidal signal becomes clearly more pronounced (Figure 4.1b). This is particularly true for the flood tide velocities (negative values), although the absolute tidal velocities remain low (maximum ca 0.11 m s^{-1} in both scenarios). In lower San Tomás Aquino Creek, the reconnections cause a smaller increase in the flow velocities during high river discharges (maximum a factor of 3; Figure 4.2a) than in lower Calabazas Creek. Furthermore, the increase is much larger in Scenario B compared to Scenario A. This also applies to the flood and ebb flow velocities displayed in Figure 4.2b. For both Calabazas and San Tomás Aquino Creeks, the differences in the tidal flow velocities between the reference case and the two scenarios become smaller moving upstream and are negligible around Highway 101 (see Figure 3.1b for the location).

The increase in flow velocities in the lower Calabazas and San Tomás Aquino Creeks in the reconnection scenarios has a clear impact on the simulated sediment transport and morphodynamics in the study area. As a result of the higher flow velocities, suspended sediment transport also becomes larger in both creeks (Figure 4.3). This effect is particularly pronounced in lower Calabazas Creek (more than a factor of 6) where a stronger increase in the flow velocities is also observed (see above). The increase in the flood and ebb flow velocities, however, is too small to be reflected by the suspended sediment transport in both creeks.

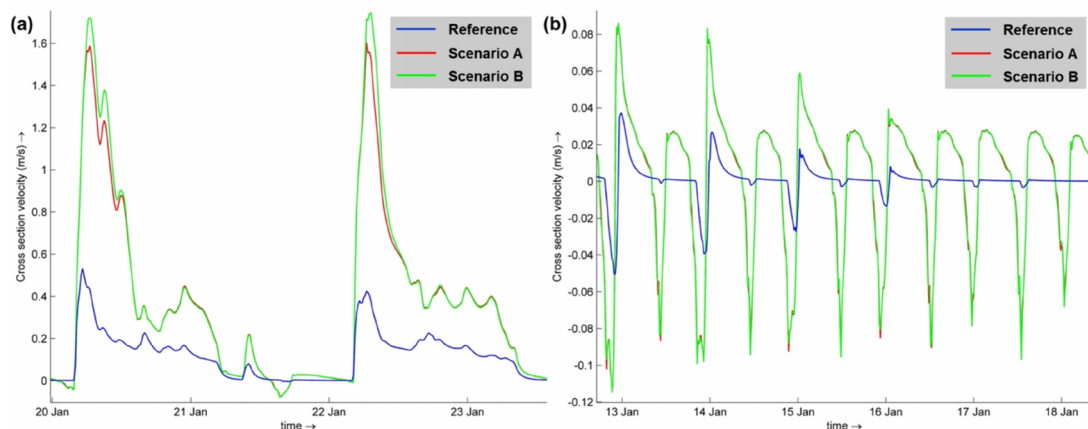


Figure 4.1: Depth averaged flow velocities simulated at cross section Cal in the reference case, and Scenarios A and B. Cross section Cal is located at the downstream end of Calabazas Creek (Figure 3.3). The left diagram (a) shows the simulated flow velocities during three high river discharge events in January 2017. Earlier in January 2017, no discharge occurred and the flow is dominated by the tide (right diagram, (b)). Positive velocities indicate downstream flow; negative velocities are upstream flow, which occurs during flood tide when river discharge is low.

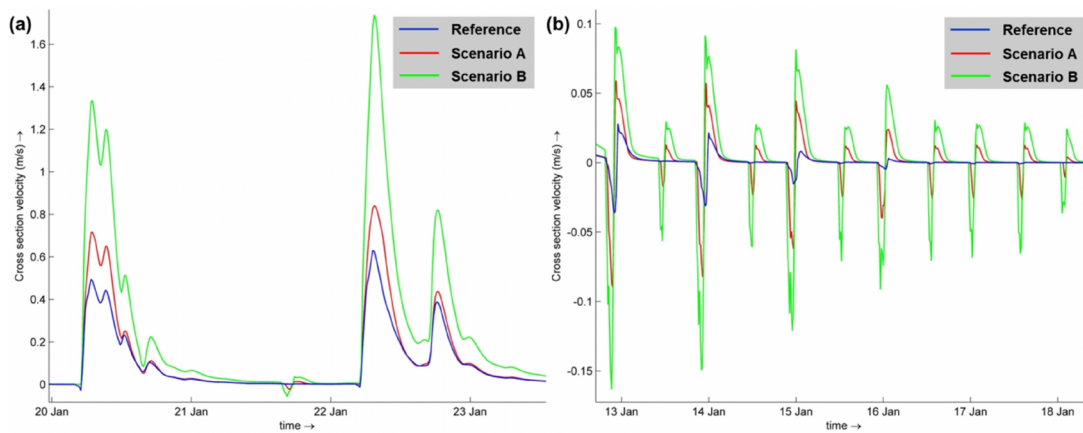


Figure 4.2: Depth averaged flow velocities simulated at cross section STA in the reference case, and Scenarios A and B. Cross section STA is located about 600 m to the east of the confluence of Calabazas and San Tomás Aquino Creeks (Figure 3.3). The left diagram (a) shows the simulated flow velocities during two high river discharge events in January 2017. Earlier in January 2017, no discharge occurred and the flow is dominated by the tide (right diagram, (b)). Positive velocities indicate downstream flow; negative velocities are upstream flow, which occurs during flood tide when river discharge is low.

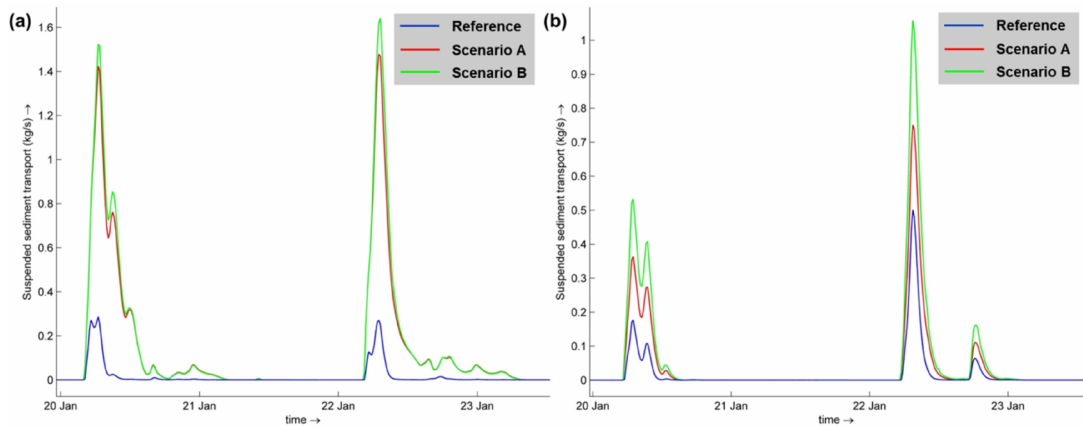
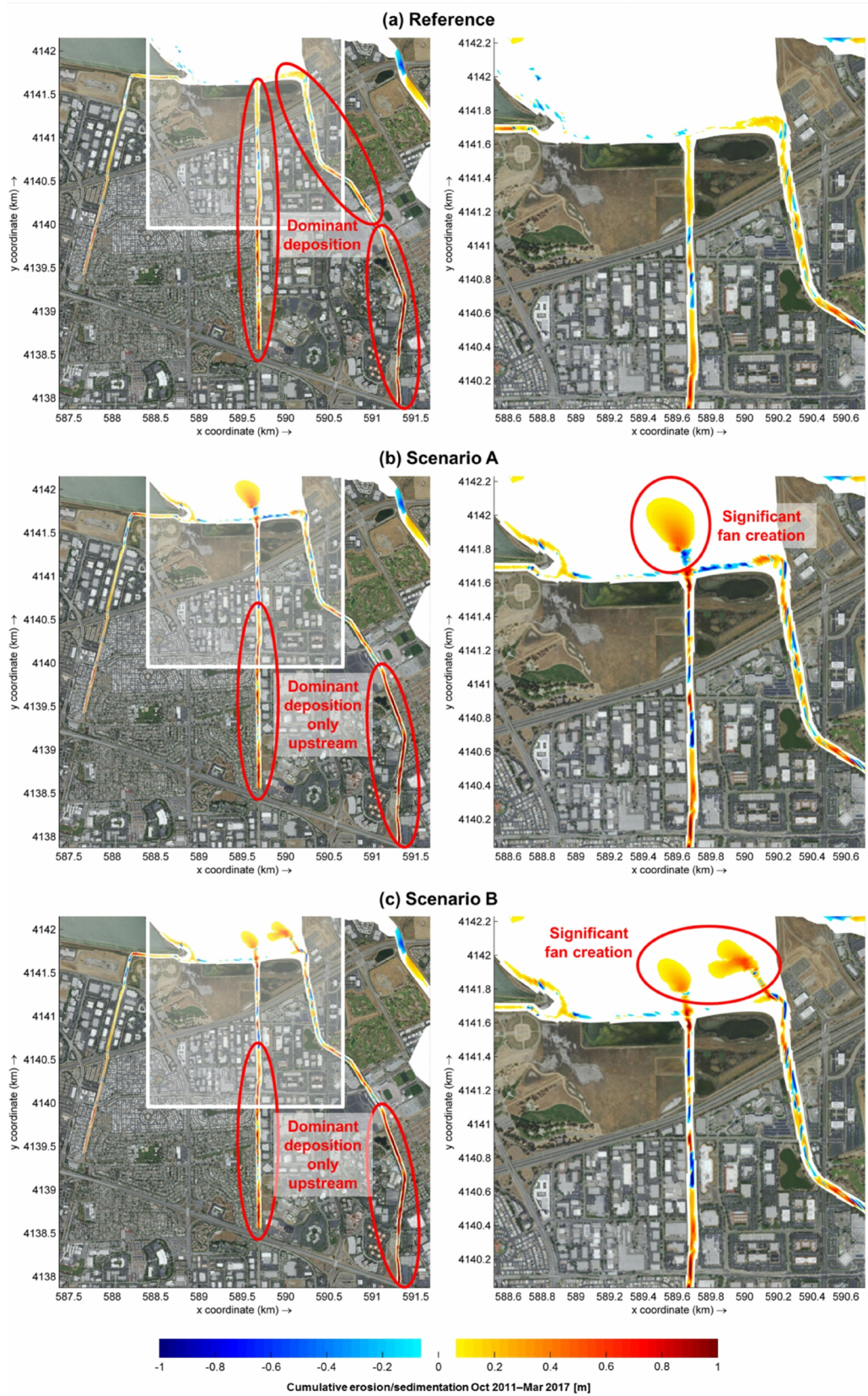


Figure 4.3: Suspended sediment transport through cross sections Cal (a) and STA (b) simulated for the reference case, Scenarios A and B during three high river discharge events in January 2017. For the locations of the cross sections see Figure 3.3a.

Figure 4.4 shows the cumulative erosion and sedimentation, i.e. the absolute bed level changes, after 5 ½ years for the reference case (Figure 4.4a) and the two reconnection scenarios (Figure 4.4b and c). In all three simulations the bed level changes do not exceed ± 1 m in the study area. For the reference case, Calabazas and San Tomás Aquino Creeks are generally dominated by sediment deposition (Figure 4.4a). Sedimentation is particularly pronounced – on the order of 1 m – in the up-stream half of both creeks but decreases in a downstream direction. The strong sedimentation in the upstream parts of the creeks can also

Figure 4.4: Simulated cumulative erosion and sedimentation after 5 ½ years for the reference case (a), and reconnection Scenarios A (b) and B (c). In the reference case, both the entire Calabazas and San Tomás Aquino Creeks are generally dominated by deposition, while deposition in the reconnection scenarios only dominates in the up-stream parts of both creeks. Note that significant sediment fans develop to the north of the levee breaches in Scenario A and B.



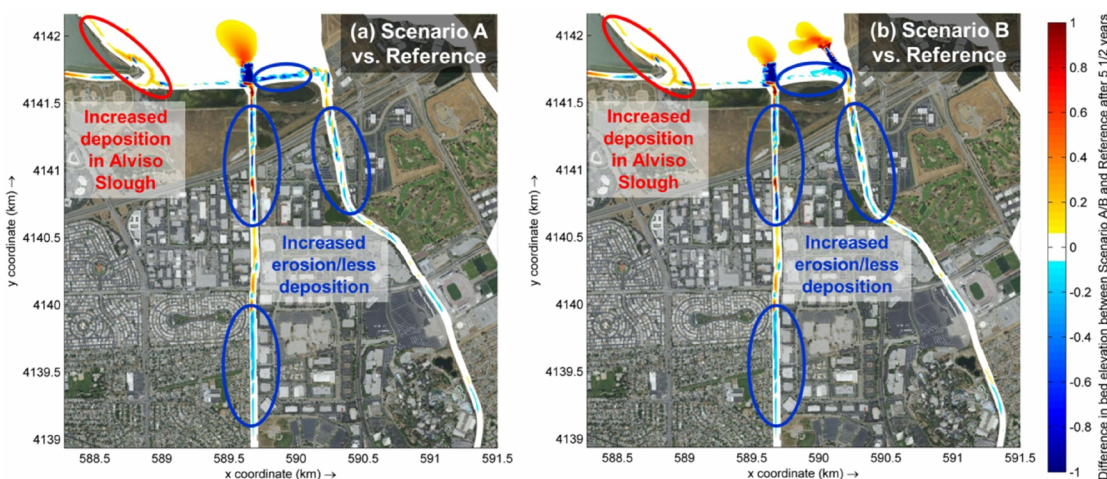


Figure 4.5: Differences in the bed elevation after 5 ½ years between Scenario A and the reference case (a) and between Scenario B and the reference case (b). Blue colours indicate lower bed elevations (i.e. increased erosion/less deposition) in the scenarios compared to the reference case at the end of the simulations after 5 ½ years, while yellow to red colours mark higher bed elevations (i.e. less erosion/increased deposition) in the scenarios compared to the reference case. Both scenarios are characterised by increased erosion/less sedimentation in the creeks compared to the reference case. Note that the dark blue colours directly south of the sediment fans in (a) and (b) are related to the implementation of the breaches in the model.

be observed in both reconnection scenarios (Figure 4.4b and c). Further downstream, however, alternating sections of significant erosion and sedimentation appear which are in contrast to the general sedimentation recorded for this area in the reference case. This erosion-sedimentation pattern results from a smoothing process of the creek bathymetries in the model associated with the increased flow velocities. A striking morphodynamic process in both scenarios is the fan creation to the north of each of the breaches connecting the creeks with Pond A8 (Figure 4.4b and c). The fans have a diameter of more than 300 m and a maximum thickness of about 0.8 m.

The described variations in the erosion-sedimentation pattern between the reference case and the scenarios result in distinct differences in the final simulated bed elevations. This becomes obvious from Figure 4.5, which shows the differences in the bed elevations after 5 ½ years between Scenario A and the reference case (Figure 4.5a), and between Scenario B and the reference case (Figure 4.5b). Besides the increased bed elevation in the area of the sediment fans, both scenarios generally show lower bed elevations at the end of the simulations than the reference case. This is particularly true for the downstream parts of both creeks where the differences in the bed elevations locally reach 1 m. The lower bed elevations indicate increased erosion or less deposition in the scenarios compared with the reference case. This can be explained by the larger flow velocities and corresponding increased transport capacity that is especially prevalent in the downstream parts of the creeks in both scenarios (see above). Finally, greater sedimentation occurs downstream of the confluence of Calabazas and San Tomás Aquino Creeks in the Alviso Slough in the reconnection scenarios (Figure 4.5). This is related to a decrease in the flow velocities in this part of the creek system, since more water is directly discharged through the breach(es) into Pond A8.

5 Discussion and conclusions

The simulation results of the current study demonstrate that both reconnection scenarios for Calabazas and San Tomás Aquino Creeks have a significant impact on the local hydro- and morphodynamics. The reconnections result in a strong increase in the tidal signal and in the downstream flow velocities during high river discharge events. While the flood and ebb flow velocities remain relatively low (maximum 0.15 m s^{-1}), flow velocities during high discharges reach values of almost 1.8 m s^{-1} once the creeks are reconnected to Pond A8. This is related to the vertical shift of the local base level of the creeks, which becomes lower due to the breaching. Furthermore, there is less backwater in the creek system in the reconnection scenarios because more water is directly discharged through the breach(es) into Pond A8 (especially during low tide). These effects are especially pronounced in Scenario B due to the double breaching. As a consequence, the increase in the flow velocities is larger in Scenario B compared to Scenario A.

As demonstrated in the results chapter (Chapter 4), the larger flow velocities in the reconnection scenarios are directly linked to an increase in the sediment transport capacity in both creeks, which in turn causes more erosion/less deposition in the creeks. As the initial sediment loads at the upstream boundaries of both creeks are the same in the reference case and the two scenarios (see Chapter 3), the stronger erosion/reduced sedimentation in the creeks indicate an increase in the sediment export by both creeks in the reconnection scenarios. Based on the higher flow velocities and larger sediment transport in Scenario B, it can be assumed that also the sediment export is larger in this scenario. Directly to the north of the breaches, flow divergence and, related to this, a decrease in the local sediment transport capacity causes the creation of significant sediment fans. Due to the double breaching in Scenario B, here, the released sediment is distributed over a larger area and the sediment fans become less thick compared to Scenario A. Both, the stronger erosion/reduced sedimentation in the creeks as well as the fan creation are morphodynamic processes which – although less pronounced – can also be observed in the short-term simulations with a duration of $1 \frac{1}{2}$ years.

The larger flow velocities during high discharges in Calabazas and San Tomás Aquino Creeks in the reconnection scenarios can be assumed to reduce the regional flooding risk originating from creek discharge. Furthermore, the indicated increase in sediment export by the creeks may lead to the conclusion that the breaching reduces the dredging volumes especially in the lower creeks, which are currently required to maintain the flow capacity and to avoid flooding in the winter season. However, further simulations have to be performed in order to make more reliable and quantitative predictions on the hydro- and morphodynamic impact of the various reconnection scenarios and on the expected future flooding risk and required dredging volumes. Such simulations should particularly consider (i) more sensitivity analyses in terms of various model parameters, as for instance bed roughness, initial sediment thickness and initial sediment loads at the upstream boundaries of the creeks, (ii) additional constituents, e.g. salinity and multiple sediment fractions, (iii) the role of vegetation, especially in the area of the sediment fans, (iv) additional breaching scenarios, e.g. diagonal connection between San Tomás Aquino and Calabazas Creeks, (v) longer simulation times (up to several decades) in order to gain greater insight into long-term morphological changes, and (vi) climate change, with a focus on the sea level rise and the potential increase in high river discharge events.

References

- Deltares. 2016. D-Flow Flexible Mesh. User manual. Version 1.1.0. http://oss.deltares.nl/documents/637298/641496/D-Flow_FM_User_Manual.pdf. 2017-12-01.
- FOXGROVER, A.C., HIGGINS, S.A., INGRACA, M.K., JAFFE, B.E. & SMITH, R.E. 2004. Deposition, erosion, and bathymetric change in South San Francisco Bay: 1858–1983. U.S. Geological Survey Open-File Report, **2004-1192**. <http://pubs.usgs.gov/of/2004/1192>. 2017-12-22.
- FOXGROVER, A.C., DARTNELL, P., JAFFE, B.E., TAKEKAWA, J.Y. & ATHEARN, N.D. 2007. High-resolution bathymetry and topography of south San Francisco Bay, California. U.S. Geological Survey Scientific Investigations Map, **2987**. <http://pubs.usgs.gov/sim/2007/2987>. 2017-12-22.
- FOXGROVER, A.C., FINLAYSON, D.P., JAFFE, B.E. & FREGOSO, T.A. 2014. Bathymetry and digital elevation models of Coyote Creek and Alviso Slough, South San Francisco Bay, California. U.S. Geological Survey Open-File Report **2011-1315**. doi: 10.3133/ofr20111315.
- REY, C. 2015. Mud dynamics in a tidal channel: The impact of opening salt ponds on channel deepening. Master thesis WSE-HECEPD-15.08, UNESCO-IHE Institute for Water Education.
- SHELLENBARGER, G.G., DOWNING-KUNZ, M.A. & SCHOELLHAMER, D.H. 2015. Suspended-sediment dynamics in the tidal reach of a San Francisco Bay tributary. *Ocean Dynamics*, **65**, pp. 1477–1488. doi: 10.1007/s10236-015-0876-0.
- VAN RIJN, L. 1993. Principles of sediment transport in rivers, estuaries and coastal seas. Aqua Publications, Amsterdam.